ISSN 1213–2489
e-ISSN 2787–9402

DOI: 10.21062/mft.2023.076 http://www.journalmt.com

Predictive Modelling On Machining Performance of ECDM Using Artificial Neural Network and Particle Swarm Optimization

Nuraini Lusi (0000-0001-9113-4976)[1], Anggra Fiveriati (0000-0003-3105-2922)[1], Akhmad Afandi (0000-0002-3518-9478)[1], I Gusti Ngurah Bagus Catra Wedarma (0000-0002-1273-6811)[1], Herman Yuliandoko (0000-0002-0449-8104)[2], Mahros Darsin (0000-0002-4254-8969)[3], Syed Qutaba (0000-0003-2328-0466)[4]
[1]Department of Mechanical Engineering, Politeknik Negeri Banyuwangi, 68461 Banyuwangi, Indonesia
[2]Department of Informatic Engineering, Politeknik Negeri Banyuwangi, 68461 Banyuwangi, Indonesia.
[3]Department of Mechanical Engineering, University of Jember, Jalan Kalimantan 37 Jember 68121, Indonesia
[4]Department of Textile, BUITEMS, Quetta 87100, Pakistan
Corresponding's Author Email: nurainilusi@poliwangi.ac.id

The electrochemical discharge machining (ECDM) process is developing into a potentially useful method of performing machining in conductive or non-conductive materials. The experiment was conducted utilizing full factorial design (2^4) with the 16 run test. The present study implemented artificial neural network (ANN) and particle swarm optimization (PSO) techniques to predict the Material Removal Rate (MRR) and surface roughness (SR), and the linear regression analysis were utilized for this purpose. The input parameters were adjusted with the objective of maximizing the MRR and minimizing the SR. The four selected process parameters are voltage, gap width, electrode type, and type of electrolyte, with each parameter has two levels, copper and brass were chosen as the electrodes in this particular technique. Linear regression (LR) modelling was calculated for comparison between the ANN model and LR. Artificial neural network (ANN) models have been developed to accurately predict SR and MRR, achieving a prediction accuracy of over 90%. The impacts of these findings have great significance for the future of machining tungsten carbide utilizing ECDM. Based on the results of R^2, the modelling with ANN is closer to the actual value than the prediction using a linear regression model, the value of R^2 ANN greater than LR so that the prediction model of ANN is still the best model.

Keywords: ANN, particle swarm, ECDM, Surface roughness, Tungsten Carbide.

1 Introduction

Electrochemical discharge machining (ECDM) is an innovative manufacturing technique that integrates the principles of electrochemical machining (ECM) and electrical discharge machining (EDM). This advanced method enables the precise fabrication of micro-scale components, including micro holes, microchannels, micro grooves, and intricate three-dimensional structures, in conductive and non-conductive materials. ECDM, an abbreviation for electrochemical discharge machining and electrical discharge machining, offers tremendous potential for enhancing the manufacturing process in various industries and has become a focal point of research and development [1–3]. Electrochemical discharge machining (ECDM) is a highly versatile manufacturing technique that enables the precise machining of a wide range of materials, including metals, superalloys, ceramics, glasses, and composites. These materials, characterized by their rigidity, delicacy, conductivity, and non-conductivity, can be intricately shaped using ECDM. This cutting-edge method operates by leveraging the phenomenon of electrochemical discharge that occurs near an electrode. With its ability to achieve exceptional precision and control, ECDM has emerged as a significant area of focus in research and development for various industries. In this process, a small tool electrode is employed to carry out the machining operations. In ECDM, each electrode is partially submerged in a suitable electrolyte solution. A holder is used to clamp the workpiece, and then the workpiece is positioned such that it is below the tool electrode. The tool electrode is then placed in an area where it is only partially submerged in the electrolyte. Due to the size disparity between the tool and auxiliary electrodes, the auxiliary electrode is often substantially more significant than the tool electrode. The introduction of a direct current supply voltage to both electrodes caused a change in dimension, which ultimately results in the production of a potential gap between the two electrodes. This difference in potential is the critical component that kickstarts the electrolysis process and causes the reaction. When the voltage between the tool electrode and the workpiece is higher than a predetermined critical voltage, the electric discharge will occur [4].

Multiple parameters affect the complexity of the machining process while using ECDM. Numerous research studies carried out the ECDM process characteristics. The ECDM process is a complex process that generates many process parameters, and it plays an essential role in the quality characteristics of ECDM machining. It focuses on the type of material, electrolyte fluid, machining quality, electrode characteristics, and gas film formation [5]. Voltage [6], the tool gap electrodes [7], pulse duty cycle [8], a current signal [9], polarity [10], feed rate, tool material, electrolyte properties[10, 11] are have been investigated for their influence on response in the ECDM process to obtain the optimum response. The quality characteristics studied focused on surface roughness [12, 13], material removal rate (MRR) [14], tool wear ratio [3], and overcut [15].

Jawalkar et [16] al studied the different electrolyte NaOH and NaCl in enhancing metal removal rate. The researcher observed a significant disparity in the rate of material extraction between NaCl and NaOH, with NaCl exhibiting a notably slower rate compared to NaOH, as revealed by the study's findings. Furthermore, during the research, it was observed that elevating the voltage to 70 volts and augmenting the electrolyte concentration to 22% resulted in a higher material removal rate when employing NaCl solution as compared to NaOH solution. This significant finding underscores the influence of voltage and electrolyte concentration on the effectiveness of material removal during the experimentation The tool electrode was made of stainless steel. Achieving the best quality targets in ECDM process is quite challenging due to the complexity it has. Therefore, it is necessary to determine the appropriate parameter combination settings through experiments with optimization methods. An experimental study using the Taguchi method was carried out on the ECDM process of soda-lime glass material; the responses studied were tool wear and MRR [17–19]. The electrodes used are copper and stainless steel and NaOH electrolyte. The experiment was carried out based on the L^4 orthogonal array. Experimentally, all the selected parameters were significant, and the wear of the copper tool was higher than that of stainless steel. Antil et al. [20] have predicted and optimized the MRR and taper of the SiC (silicon carbide) using full factorial design and a neural network-based hybrid model. Regression analysis and artificial neural network (ANN) have been recommended by a researcher [21] to predict the MRR of Soda-lime glass. Demonstrate a harmonious alignment between the experimental outcomes and the projected model. Notably, artificial neural network (ANN) models have been extensively employed in assessing the impact of diverse machining parameters in different non-conventional machining methods and in predicting optimal process parameter values or predicting process performance measures. This substantiates the widespread use and versatility of ANN models in predicting and optimizing various aspects of machining processes [22–27] .

The utilisation of predictive techniques in the modelling and optimising parameters in modern machining processes has emerged as a significant milestone for the manufacturing industries. This development signifies a pivotal advancement in the field, allowing for the precise and efficient determination of optimal process parameters. By employing these sophisticated optimisation techniques, manufacturing industries can enhance their productivity, quality, and overall operational performance. This breakthrough holds tremendous potential for revolutionising manufacturing practices and driving substantial improvements in the efficiency and effectiveness of machining processes. As a result, numerous researchers are attempting to make use of these advanced optimization techniques for a variety of different processes [28]. Several researchers have used various optimization methods, such as Taguchi's methodology [7], response surface methodology [8], artificial neural network [9] and grey relational analysis [10], genetic algorithm [29, 30], particle swarm optimization [31, 32], etc., to optimize the machining processes for single and multi-response.

The demand for the manufacture of tungsten carbide products is a challenge due to its high strength. Many metal compounds are used in industry, but none of the materials has tungsten carbide's unique properties. The combination of carbon and tungsten elements produces a super hard metal alloy similar to diamond that has resistance to heat, friction, scratches, corrosion, and high fatigue [33]. Tungsten carbide is recently used as a cutting tool for turning and milling processes, dies production, and mould maker. The use of tungsten carbide is not limited only to the manufacturing industry but also to the medical components, such as surgical instruments and implants. The hardness of tungsten carbide is two times greater than the hardness of steel, and since tungsten carbide is typically difficult-to-cut material, it isn't easy to be machined. Innovation in metal cutting processes such as hybrid manufacturing-based technology is independent of the hardness of the workpiece [34, 35]. This technology is an innovation to reduce machining costs, increase machining speed, quality and capability to manufacture complex shapes of various components that traditional machining cannot produce economically [36]. The unconventional machining process is more promising due to its versatility and controlled parameters, and most of the techniques use thermal energy for its mechanism [37]. This present study aims to investigate the parameters of the ECDM process of tungsten carbide (WC) to achieve minimum surface roughness and maximum surface roughness. The full factorial design chosen as an experimental design and predicting modelling using ANN was used to determine the minimum surface roughness.

2 Materials and Methods

2.1 Equipment of Experimentation

Experiments performed on the fabricated ECDM prototype model include various components, consisting of machining control based on the Arduino system, a single Z-axis linear motion to feed the tool, spindle, a fixture for the workpiece, an acrylic material as an electrolyte chamber, a circulation pump electrolyte immerse, and electrical system with DC power. Tungsten carbide (WC) dimensions 19 mm x 17 mm with 4 mm thickness as an anode workpiece. Two types of cylindrical cathode tools used were copper and brass with a diameter of 13 mm and had 80 mm in length, and an auxiliary anode was stainless steel. The experimental setup shows in Fig. 1. The condition of the machining is shown in Table 1.

***Tab. 1** The experimental machining condition*

Machine	Fabricated prototype ECDM Set-up
A voltage of DC supply	0-120 V
Current	0-15 A
Cathode tool	Copper and Brass
Auxiliary electrode	Stainless steel (L-100 mm)
Electrolyte and concentration	NaCl and NaNO3
Anode workpiece	Tungsten carbide
Level of Electro-lyte	Approx. 0.5 mm above the workpiece

***Fig. 1** An ECDM process setup*

2.2 Machining parameters of ECDM

In this experimental design, four factors with two levels were selected based on literature and experts, namely voltage, type of electrode, type of electrolyte, and gap width. Furthermore, a factorial design of two levels (2^4) is applied, as shown in Table 2.

***Tab. 2** ECDM input parameters*

Input Factors	Units	Role	Maximum Value	Minimum Value
Voltage	Volt	Continous	70	90
type of electrode	-	Categorical	Copper	Brass
type of electrolyte	-	Categorical	NaCl	$NaNO_3$
gap width	mm	Continous	1	2

2.3 Design of Experiments

Based on the experimental design, 16 tests were run and conducted in two replications. The surface roughness test was carried out using Mahr Marsurf RD 18 instrument. The surface roughness is obtained from the machining process results based on parameters that have been determined respectively, as shown in Table 3.

***Tab. 3** Result of the measurement*

Number of Trials	Voltage	Gap width	Electrode	Electrolyte	MRR actual (g/min)	Surface Roughness (μm)
1	70	1	Brass	NaCl	0.016	0.68
2	90	1	Brass	NaCl	0.027	0.93
3	70	2	Brass	NaCl	0.007	0.82
4	90	2	Brass	NaCl	0.014	0.91
5	70	1	Copper	NaCl	0.004	0.42
6	90	1	Copper	NaCl	0.01	0.76
7	70	2	Copper	NaCl	0.012	0.56
8	90	2	Copper	NaCl	0.026	0.52
9	70	1	Brass	$NaNO_3$	0.011	0.73
10	90	1	Brass	$NaNO_3$	0.025	0.69
11	70	2	Brass	$NaNO_3$	0.007	0.82
12	90	2	Brass	$NaNO_3$	0.028	0.94
13	70	1	Copper	$NaNO_3$	0.022	1.043
14	90	1	Copper	$NaNO_3$	0.015	1.114
15	70	2	Copper	$NaNO_3$	0.007	1.107
16	90	2	Copper	$NaNO_3$	0.033	1.553

3 ANN-PSO Modelling

Artificial Neural Network (ANN) is an intricately designed computational framework inspired by the intricate workings of biological neural networks in the human brain. ANN models can capture and analyze intricate patterns and relationships within vast datasets. The application of ANN in various research domains and industries has led to significant advancements in data analysis, prediction, and decision-making processes. This paradigm shift in computing represents a remarkable fusion of neuroscience and technology, providing a powerful tool for solving complex problems and gaining deeper insights into complex phenomena. The utilised neural network architecture is Backpropagation (BP), a systematic approach for training in multi-layered networks. The approach utilised in this study is founded on mathematical principles, rendering it robust and impartial. The algorithms employed in this methodology are currently being refined, with equations and coefficient values incorporated into formulas aimed at minimising the sum of squared errors through the model error that was established during the training set. BPANN is a methodical approach to training multilayer neural networks, also known as multi-layered perception neurons. The first layer is made up of one input set, and the last layer is the output (goal) that should be achieved. The neural network architecture typically includes an intermediate layer, commonly referred to as the hidden layer, situated between the input and output layers. In practical application, the quantity of hidden or potential variables is subject to variation. The maximum number of layers is three. The input layer of a neural network represents the input variable, while the hidden layer introduces non-linearity to the network system. Within the neural network architecture, the output layer is responsible for selecting the output variables. In contrast, the last layer of the hidden layer functions as the immediate output of the neural network. In other words, the output layer acts as the final computation stage, producing the desired results or predictions based on the input data. This distinct layer plays a critical role in conveying the processed information from the hidden layers to generate the final output. The significance of this arrangement lies in its ability to transform complex computations and transformations performed within the hidden layers into meaningful and actionable outcomes. Therefore, the output layer is pivotal in the neural network's ability to provide accurate and valuable insights or predictions based on the input.

Modelling the experimental data using the ANN approach allows for the study of the effect that the input parameters have on the surface roughness and the metal removal rate. These input parameters include voltage, electrode, electrolyte, and gap width. The BP training process involves three stages: feedforward data input, backpropagation for error values, and weight value adjustments for each node in the ANN's layers. The method of trial and error has been used by a number of researchers in order to determine the network architecture in order to obtain the best model [38]. As a result, there is no definitive rule that can be used to determine it apart from experimentation. The artificial neural network (ANN) utilised in this investigation had just one input layer, one hidden layer, and one output layer, as shown in Fig. 2 and 3, respectively. Four neurons are located in the input layer of MRR and SR's neural network, whereas nine are located in the hidden layer, and one is located in the output layer.

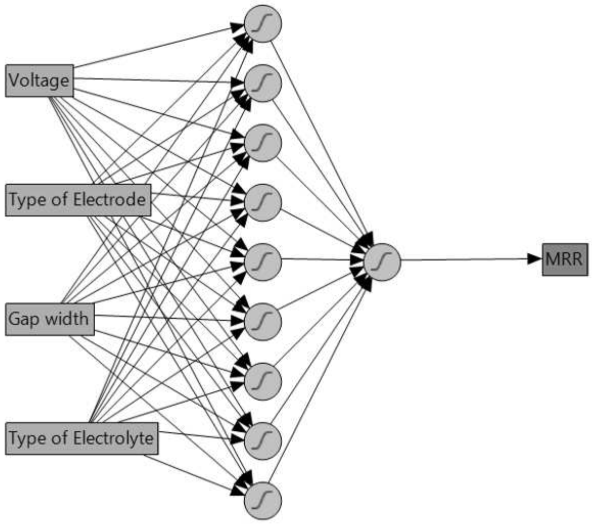

Fig. 2 *Architecture of predictive model of MRR*

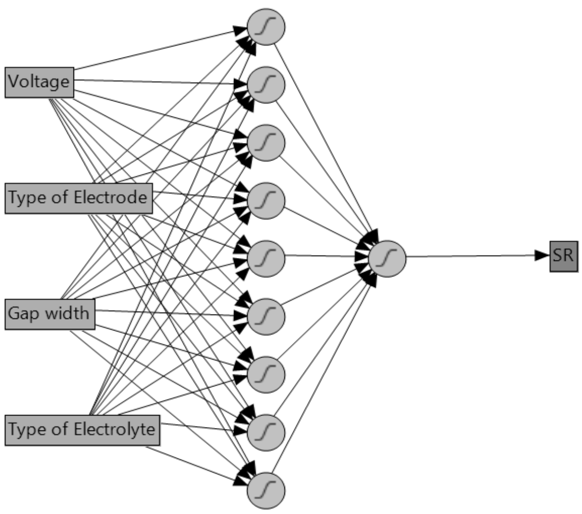

Fig. 3 *Architecture of predictive model of SR*

Equation 1 is used in conjunction with the prediction error per-centage equation to determine the percentage of incorrect predictions that were successful [39].

$$\% \, error = \frac{|Exp - Pred|}{Exp} x100 \qquad (1)$$

Model performance is evaluated to measure the accuracy of a model. Assessing model performance is a crucial aspect of constructing predictive models. This study employs a performance model to evaluate the relationship between observed data and predicted outcomes. The benchmark correlation coefficient is used for this objective. Mean Absolute Deviation (MAD Mean Squared Error (MSE), Root Mean Squared Error (RMSE), and Mean Absolute Percentage Error (MAPE) are frequently used model performance evaluations. The current study entails the calculation of the Mean Square Error (MSE) metric, a quantitative measure that evaluates the average discrepancy between predicted and actual values. This metric is an essential tool for assessing the accuracy and precision of predictive models by quantifying the extent of deviation between predicted and observed outcomes. By computing the MSE, researchers can gain insights into the overall performance and reliability of the model under investigation. This evaluation provides a comprehensive understanding of the effectiveness and quality of the predictions, enabling researchers to gauge the level of agreement between predicted and actual values and identify potential areas for improvement. Thus, the utilization of the MSE metric in this investigation serves as a valuable means of evaluating and quantifying the predictive capabilities of the model being studied. As the value decreases, the network error in approximating the target value also decreases. The regression coefficient is estimated to determine whether the network output adequately corresponds to the expected outcome. This helps to ensure that the network is functioning correctly. The degree of suitability is indicated by a regression coefficient that approaches unity.

3.1 Mean Absolute Percentage Error (MAPE)

In the research study, the Mean Absolute Percentage Error (MAPE) metric is employed to evaluate the average percentage deviation between predicted and actual values. This metric serves as a valuable tool for quantifying the average deviation between the predicted and observed outcomes, expressed as a percentage of the actual values. By utilizing MAPE, researchers can accurately measure the relative error between predicted and actual values, providing valuable insights into the precision and accuracy of the predictive model under investigation. This metric allows for a comprehensive understanding of the average percentage difference between predicted and actual values, enabling researchers to assess the effectiveness and reliability of the model's predictions. Thus, the application of MAPE in this research article plays a crucial role in quantifying and assessing the model's predictive performance. A lower MAPE value is indicative of a higher quality model [40]. Similar to Equation 2, this is the form of equations used.

$$MAPE = \frac{1}{N} \sum_{t=1}^{n} \left| \frac{A_t - F_t}{A_t} \right| \qquad (2)$$

Where:
A_t…Actual;
F_t… Forecast.

3.2 Root Mean Square Error (RMSE)

The calculation of the root means square error (RMSE), which is obtained by calculating the square root of the average of the squared disparities between predicted and actual values, is included in the study article. This metric is a robust measure for quantifying the overall magnitude of errors between predicted and observed outcomes. By computing the RMSE, researchers can effectively assess the level of deviation between predicted and actual values while also considering the magnitude of these differences. The utilization of RMSE in this research article enables a comprehensive evaluation of the predictive model's performance, providing a reliable indicator of the accuracy and precision of the predictions. Therefore, the RMSE metric plays a pivotal role in quantifying and evaluating the degree of error between predicted and actual values within the study context. A lower value of RMSE indicates a higher quality of the model, calculated by using Eq.3 [41].

$$RMSE = \sqrt{\frac{\sum_{t=1}^{n}(A_t - F_t)^2}{n}} \tag{3}$$

Where:
A_t…Actual;
F_t…Forecast.

3.3 Mean Square Error (MSE)

The Mean Squared Error (MSE) is a statistical metric that is utilized in the process of evaluating the level of precision possessed by a model. It involves squaring the difference between each data point in an array and the corresponding predicted value, summing the squares, and then calculating the average or median value. For the relevant equations, see Eq. 4.[42, 43].

$$MSE = \frac{\sum_{t=1}^{n}(A_t - F_t)^2}{n} \tag{4}$$

Where:
A_t…Actual;
F_t…Forecast.

3.4 The mean absolute deviation (MAD)

The mean absolute deviation (MAD) is calculated in the research study by adding the absolute differences between the values collected and those estimated. After that, the average deviation is calculated by dividing this quantity by the total number of observations. The mean absolute deviation, often referred to as the standard deviation, serves as a metric for quantifying the dispersion or variability of the data points. By calculating the MAD, researchers can assess the average magnitude of the deviations between actual and estimated values. This measure provides valuable insights into the spread or dispersion of the data, allowing for a comprehensive understanding of the variability present in the dataset. Therefore, using mean absolute deviation as a measure of dispersion plays a crucial role in evaluating and quantifying the level of variability within the research study. Equation 5 contains the equations that were worked with [44]. Fig. 4 show the flowchart of ANN modelling.

$$MAD = \frac{\sum_{t=1}^{n}|A_t - F_t|}{n} \tag{5}$$

Where:
A_t…Actual;
F_t…Forecast.

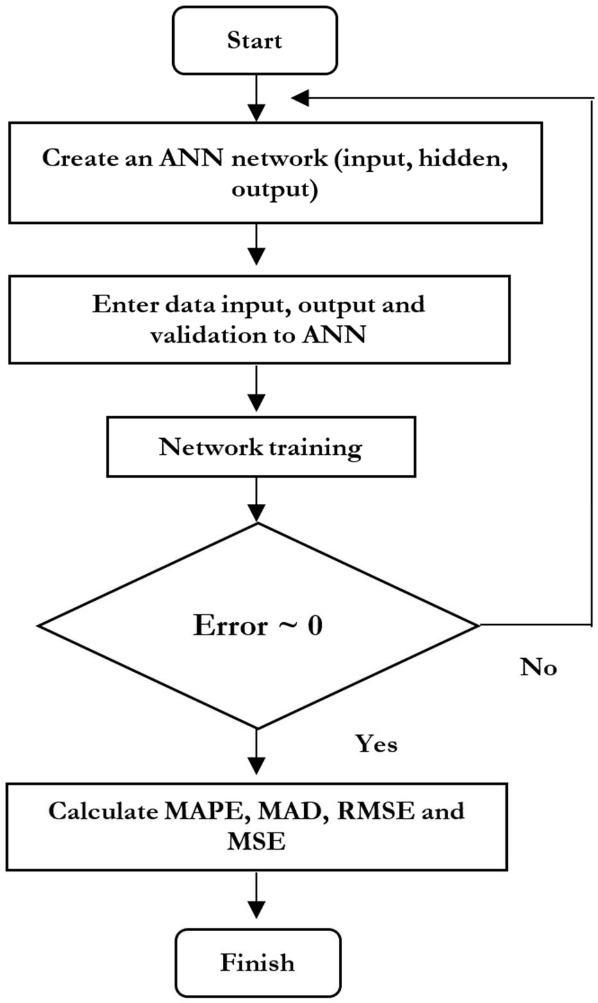

Fig. 4 *Flowchart of ANN Modelling*

An optimization technique called PSO imitates the social behavior of flocks of birds on the hunt for food. Individual acts and the impact of individual behavior on the herd make up social behavior. A bird in a flock is represented by the word particle. The other birds in the flock will be able to fly directly there if a bird locates a spot for a food supply. The initial position of each particle in the PSO algorithm is arbitrary. It is considered that each particle has two characteristics: location and velocity. A population made up of many particles searches for a solution using the PSO method. With the smallest and largest value limits, the population is produced at random. Each particle stands for a viewpoint or resolution to the current issue. By navigating the search space, each particle looks for the best answer. In order to accomplish this, each particle must adjust both its personal best position and the global best position of the entire herd as it moves over the search space. During the search for a solution, experience or knowledge is shared both within the particle and between it and the most effective particles from the entire swarm. Then, until a location that is almost the same is attained or a predefined iteration limit is reached, the search procedure is carried out to identify the optimal position for each particle in a specific number of iterations. By inserting the solution into the fitness function, each solution, which is represented by the particle position, will be assessed for its effectiveness at each iteration. The conceptual underpinning for optimization methods is shown in Fig. 5. The process parameters obtained from PSO optimization and the predicted response using an artificial neural network are shown in Table 4.

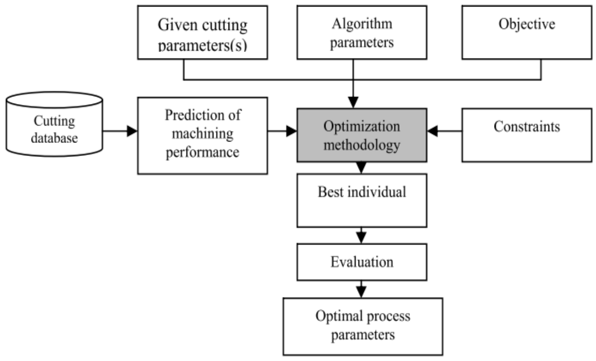

Fig. 5 *Optimization concept framework with the PSO method [45]*

Tab. 4 *Result of ANN PSO Optimization*

Exp. No	MRR (g/min)	Surface Roughness (µm)	MRR		Surface Roughness	
			Logsig	ANN-PSO	Logsig	ANN-PSO
1	0.016	0.68	0.032	0.016	0.638	0.677
2	0.027	0.93	0.004	0.027	0.997	0.929
3	0.007	0.82	0.029	0.007	0.841	0.823
4	0.014	0.91	0.024	0.014	0.657	0.908
5	0.004	0.42	0.043	0.004	0.541	0.425
6	0.01	0.76	0.024	0.010	0.550	0.754
7	0.012	0.56	0.038	0.012	0.654	0.557
8	0.026	0.52	0.031	0.026	0.626	0.526
9	0.011	0.73	0.001	0.011	0.657	0.734
10	0.025	0.69	0.009	0.025	1.147	0.684
11	0.007	0.82	0.025	0.007	0.749	0.820
12	0.028	0.94	0.015	0.028	1.077	0.943
13	0.022	1.043	0.008	0.022	1.253	1.038
14	0.015	1.114	0.013	0.015	1.101	1.121
15	0.007	1.107	0.027	0.007	1.057	1.107
16	0.033	1.553	0.032	0.033	1.504	1.544

4 Result and Discussion

Fig. 6 presents linear regression graphs that compare the predicted values generated by the ANN with the actual response variables, following the modelling process. In the research study, a linear equation y=1.004x-0.000005 was utilized, and the obtained regression coefficient (R) for the validation dataset was 0.9998. This high number for the regression coefficient indicates a significant correlation between the experiments' results and the neural network output. Additionally, the regression models were defined for the geometrical properties, and the correlation coefficients obtained were found to be satisfactory [46].

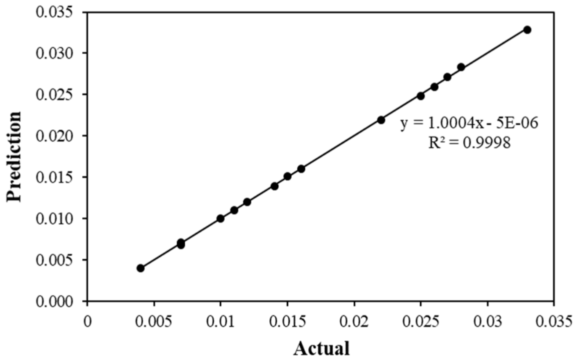

***Fig. 6** Actual vs. prediction of material removal rate of ANN model*

A linear regression model was employed to plot the Material Removal Rate (MRR) values obtained from experimental data alongside the predictions. The comparison revealed that the predictions generated by the Artificial Neural Network (ANN) exhibited closer proximity to the actual values compared to the predictions made by the linear regression model. It is vital to calculate key metrics such as mean absolute percentage error (MAPE), mean square error (MSE), mean absolute deviation (MAD), and root mean square error (RMSE) for both the actual and predicted values in order further to analyse the accuracy and performance of the predictions. These metrics include mean absolute percentage error (MAPE), mean square error (MSE), mean absolute deviation (MAD), and root mean square error (RMSE). These metrics provide a comprehensive assessment of the level of deviation and overall quality of the predictions. By quantifying the discrepancies and measuring the effectiveness of the predictive models, researchers can obtain valuable insights into the accuracy and reliability of the ANN predictions compared to the linear regression predictions, as stated in the research article [26]. The residuals, which indicate the distance between the data points and the regression line, were analyzed and documented in Table 5. By examining the residuals, researchers can assess the extent to which the data points deviate from the predicted values. The analysis of residuals provides valuable insights into the accuracy and reliability of the regression model, allowing for a comprehensive evaluation of the goodness of fit. Therefore, the examination of residuals plays a critical role in assessing the agreement between the experimental data and the predictions made by the neural network.

***Tab. 5** Calculation results of Percentage Prediction Error of MRR*

No.	Actual MRR	Prediction MRR	Residual	Percentage Prediction Error (%)
1	0.016	0.016	0.000	0.0010
2	0.027	0.027	0.000	0.0060
3	0.007	0.007	0.000	0.0046
4	0.014	0.014	0.000	0.0045
5	0.004	0.004	0.000	0.0065
6	0.01	0.010	0.000	0.0018
7	0.012	0.012	0.000	0.0016
8	0.026	0.026	0.000	0.0012
9	0.011	0.011	0.000	0.0035
10	0.025	0.025	0.000	0.0082
11	0.007	0.007	0.000	0.0264
12	0.028	0.028	0.000	0.0104
13	0.022	0.022	0.000	0.0036
14	0.015	0.015	0.000	0.0050
15	0.007	0.007	0.000	0.0157
16	0.033	0.033	0.000	0.0037

The results of e calculations are shown in Table 6. The MAPE value is 0.65 <4.9%, which can be interpreted as a surface roughness prediction obtained accurately [27]. A computed result of 0 for both the Mean Square Error (MSE) and the Root Mean Square Error (RMSE) shows that the model is very close to the actual data. This interpretation suggests that the predictions made by the model exhibit a high degree of accuracy and precision, with minimal deviation from the actual values. Similarly, for the mean absolute deviation (MAD), the result of 0.000 indicates a deficient error level. This finding signifies a high level of accuracy and reliability in the predictions, with minimal discrepancies between the predicted values and the actual data. The minimal errors and high accuracy observed in the MSE, RMSE, and MAD metrics demonstrate the effectiveness and robustness of the predictive model, further affirming the reliability of the results. These insights, as stated in the research article, underscore the model's capability to generate predictions that closely align with the actual data and emphasize the high level of accuracy achieved in the analysis.

Tab. 6 *The results of calculating the level of accuracy*

Stats Items	The calculation results
MAPE	0.65
MSE	0.000
MAD	0.000
RMSE	0.000

The linear equation y = 0.9937x + 0.0049 and the regression coefficient (R) for the validation data set that was collected were both 0.9997, which indicates that there is a good correlation between the experimental and network output. In the research article, Table 7 analyzed the residuals to determine how far the data points deviated from the regression line. The residuals quantify the extent to which the observed data points differ from the predicted values. Additionally, in Fig. 7, the linear regression model was used to plot the SR values obtained from experimental data alongside the predicted values.

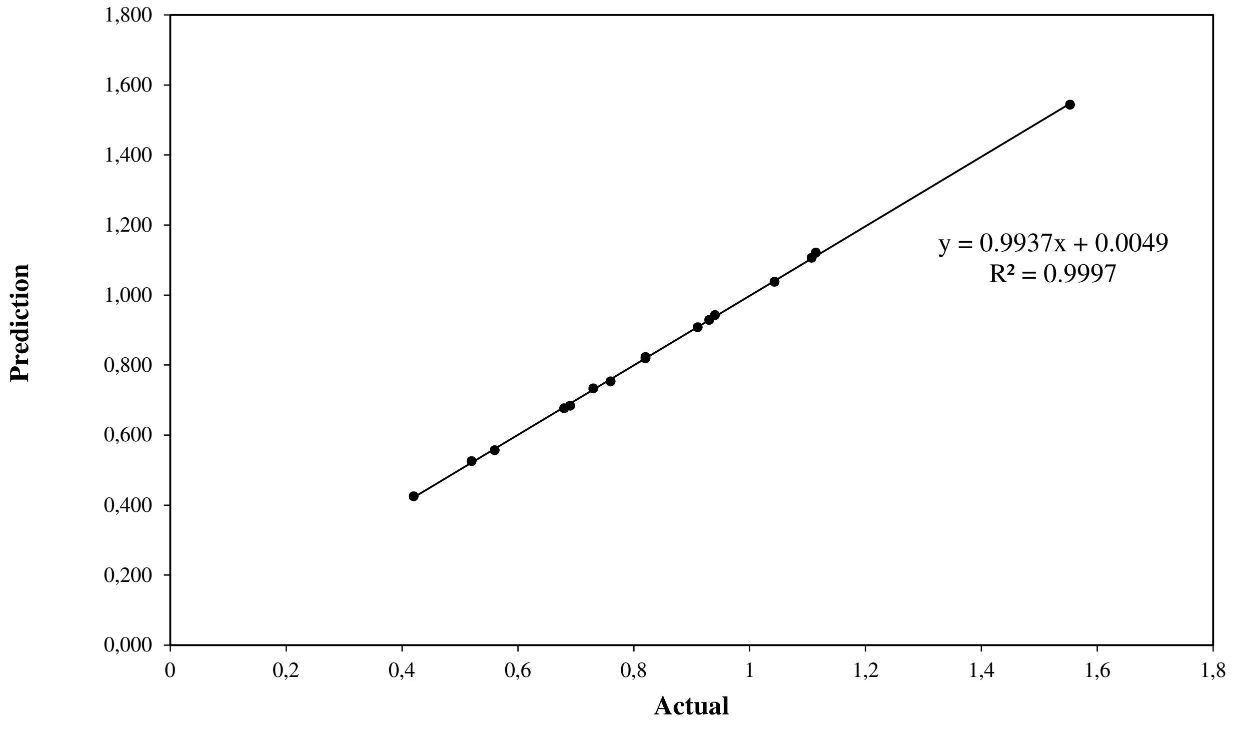

Fig. 7 *Actual vs. prediction of surface roughness of ANN model*

The comparison between the predictions generated by the Artificial Neural Network (ANN) and the linear regression model led to the inference that the ANN predictions exhibited a higher degree of proximity to the actual values than the linear regression predictions. This observation indicates that the ANN model outperformed the linear regression model regarding accuracy and precision in predicting the SR values. These findings, as stated in the research article, underscore the superior predictive capabilities of the ANN model, highlighting its ability to generate predictions that closely align with the actual values.

Tab. 7 *Calculation results of Percentage Prediction Error of SR*

No.	Actual MRR	Prediction MRR	Residual	Percentage Prediction Error (%)
1	0.68	0.677	0.003	0.0042
2	0.93	0.929	0.001	0.0008
3	0.82	0.823	-0.003	0.0033
4	0.91	0.908	0.002	0.0024
5	0.42	0.425	-0.005	0.0127
6	0.76	0.754	0.006	0.0083
7	0.56	0.557	0.003	0.0050
8	0.52	0.526	-0.006	0.0112
9	0.73	0.734	-0.004	0.0052
10	0.69	0.684	0.006	0.0089
11	0.82	0.820	0.000	0.0003
12	0.94	0.943	-0.003	0.0031
13	1.043	1.038	0.005	0.0043
14	1.114	1.121	-0.007	0.0063
15	1.107	1.107	0.000	0.0002
16	1.553	1.544	0.009	0.0058

The MAPE value is 0.51 <4.9%, which can be interpreted as a surface roughness prediction obtained accurately [27]. Regarding the Mean Square Error (MSE) and the Root Mean Square Error (RMSE), a calculated value of 0 indicates that the actual data and the anticipated values are close together. This interpretation indicates that the predictive model's performance is highly accurate, with minimal deviation from the actual values. Similarly, for the mean absolute deviation (MAD), the result of 0.004 indicates a negligible error. This outcome signifies a high level of accuracy and precision in the predictions, with minimal discrepancies between the predicted values and the actual data. The exceptionally low errors and high accuracy observed in the MSE, RMSE, and MAD metrics validate the effectiveness and reliability of the predictive model, underscoring its capability to generate predictions that align closely with the actual data. These findings, as highlighted in the research article, demonstrate the model's capacity to deliver accurate and reliable predictions, reflecting a high level of precision in the analysis. Fig. 8 and Fig. 9 each display a mean effect plot highlighting the influence of several factors on the rate of material removal and surface roughness, respectively.

Tab. 8 *The results of calculating the level of accuracy*

Stats Items	The calculation results
MAPE	0.51
MSE	0.000
MAD	0.004
RMSE	0.005

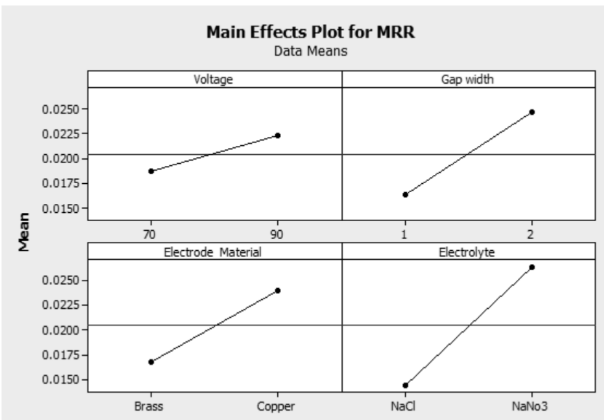

Fig. 8 *Material removal rate main effect plot*

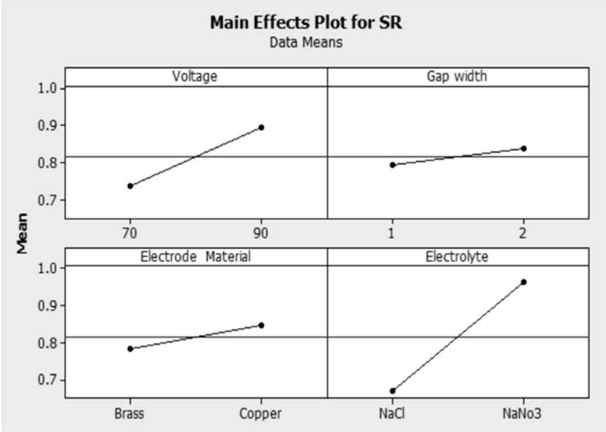

Fig. 9 *Surface roughness main effect plot*

4.1 The effect of voltage

Increasing the voltage that is applied causes a greater quantity of hydrogen gas bubbles to be formed, which results in a larger quantity of discharge energy at the parking zone. This causes the MRR and surface roughness to increase [47]. However, there is a maximum rate of material removal. A higher amount of voltage allowed the system to pour in more energy for machining, which resulted in more material being removed from the work surface and an increase in MRR and SR. Additionally, as the work-piece is struck by a greater energy spark, deeper craters will be formed, resulting in increased damage to the work surface and an increase in surface roughness [9].

4.2 The effect of gap width

The fluctuation of the machining gap, which refers to the space under at the substrate and the lower part of the tool electrode, offers a lot of positive outcomes benefits. These advantages encompass enhancing the growth of a gas film, promoting discharge activity at the tip of the tool electrode, and facilitating the flow of electrolytes beneath the tool electrode, thereby enabling chemical etching to occur more effectively [7]. Achieving precise control of the machining gap during drilling poses a significant challenge.

4.3 The effect of electrolyte

Enhancing the Material Removal Rate (MRR) in Electrochemical Discharge Machining (ECDM) can be achieved by employing a suitable electrolyte and optimizing its concentration. Electrolytes with higher pH levels exhibit an increased MRR. On the other hand, neutral electrolytes like KCl and NaCl yield a lower MRR, while acidic electrolytes such as sulfuric acid and hydrochloric acid have negligible machining effects [12]. Additionally, the MRR is influenced by the average temperature of the electrolyte. It is recommended to utilize preheated electrolytes within the range of 60 to 80°C in order to optimize MRR.

4.4 The effect of tool electrode

The performance of the ECDM is greatly influenced by the selection of the proper electrode material. Analytical concerns for optimum machining efficiency include the electrical conductivity and thermal conductivity of electrodes. Additionally, it has been demonstrated that electrical conductivity affects the MRR and surface roughness [48]. The research focused on investigating the impact of process parameters in tool electrode electrochemical discharge machining (ECDM). It noted a significant correlation between the eroded workpiece material caused by electrical discharges and the influence of ECDM process parameters. Notably, these effects were closely associated with the tool electrode utilized in machining. The study aimed to understand and analyse the intricate relationship between the ECDM process parameters, the tool electrode, and the resulting melting phenomenon of the workpiece material. By exploring these connections, researchers aimed to enhance their understanding of the underlying mechanisms governing the ECDM process and optimize the parameters for improved machining performance.

5 Conclusion

This research investigates metal removal rate and surface roughness of tungsten carbide workpieces caused by the ECDM process. Then, ANN models were created to predict the metal removal rate and surface roughness, which was dependent on ECDM parameters such as electrode material, voltage, gap width, and electrolyte. From this investigation, the following findings can be drawn:

- The ANN predictions matched the experimental values with correlation coefficients (R^2) in the range of 0.99%, mean absolute percentage errors (MPAE) in the range of 0.51-0.65 %, and extremely small root mean square errors (MSE).
- The effectiveness combination method of the artificial neural network (ANN) and particle swarm optimization (PSO) utilized to model the metal removal rate and surface roughness behaviour in the ignited tungsten carbide workpiece was examined through analysis. The outcomes show that the ANN can predict with some degree of accuracy.
- Further research is necessary to examine the potential utilization of preheating the electrolyte prior to achieving a higher material

removal rate (MRR) in the machining of tungsten carbide.

- The surface roughness of tungsten carbide during machining is mostly influenced by the voltage applied. Furthermore, it has been observed that a decrease in the voltage leads to a corresponding reduction in surface roughness.
- The findings of this current research investigation indicate that the electrochemical discharge machining (ECDM) method is a viable method for efficiently cutting hard materials. Tungsten carbide is a highly resistant material that poses challenges in terms of cutting, making it appropriate for the fabrication of dies and tooling. The utilization of an Electrochemical Discharge Machining (ECDM) method has the potential to enhance the material removal rate, as well as achieve the required levels of precision and surface finish for certain applications. Furthermore, the reduction in electrolyte loss resulted in decreased machining cost and a decrease in environmental degradation.

Acknowledgement

***The authors are grateful to the Center of Research and Community Service State Polytechnic of Banyuwangi for financial support under PB RIP grant No* 2543.22/PL36/LT/2022.**

References

[1] PAWAR P, BALLAV R, KUMAR A. Revolutionary Developments in ECDM Process: An Overview. *Mater Today Proc* 2015; 2: 3188–3195.

[2] SINGH T, DVIVEDI A. Developments in Electrochemical Discharge Machining: A Review on Electrochemical Discharge Machining, Process Variants and their Hybrid Methods. *Int J Mach Tools Manuf* 2016; 105: 1–13.

[3] BEHROOZFAR A, RAZFAR MR. Experimental Study of the Tool Wear During the Electrochemical Discharge Machining. *Mater Manuf Process* 2016; 31: 574–580.

[4] SAINI G, KUMAR A, MOHAL S, ET AL. Electrochemical Discharge Machining Process, Variants and Hybridization: A review. *IOP Conf Ser Mater Sci Eng*; 1033. Epub ahead of print 2021. DOI: 10.1088/1757-899X/1033/1/012070.

[5] SINGH L. Review on Preceding And Perspective Research In Electrochemical Discharge Machining. 2021; 1–12.

[6] KIM DJ, AHN Y, LEE SH, ET AL. Voltage Pulse Frequency and Duty Ratio Effects in an Electrochemical Discharge Microdrilling Process of Pyrex glass. *Int J Mach Tools Manuf* 2006; 46: 1064–1067

[7] MISHRA DK, PAWAR K, DIXIT P. Effect of Tool Electrode-Workpiece Gap in the Microchannel Formation by Electrochemical Discharge Machining. *ECS J Solid State Sci Technol* 2020; 9: 034011

[8] SUNDARAM M, CHEN YJ, RAJURKAR K. Pulse Electrochemical Discharge Machining of Glass-Fiber Epoxy Reinforced Composite. *CIRP Ann* 2019; 68: 169–172.

[9] ELHAMI S, RAZFAR MR. Study of The Current Signal and Material Removal during Ultrasonic-Assisted Electrochemical Discharge Machining. *Int J Adv Manuf Technol* 2017; 92: 1591–1599.

[10] KARNIK M, GHOSH A, SHEKHAR R. Polarity Dependence of The Electrochemical Discharge (ECD). *Key Eng Mater* 2011; 486: 131–134.

[11] ELHAMI S, RAZFAR MR. Application of Nano Electrolyte in The Electrochemical Discharge Machining Process. *Precis Eng* 2020; 64: 34–44.

[12] KUMAR M, VAISHYA RO, SURI NM, et al. An Experimental Investigation of Surface Characterization for Zirconia Ceramic Using Electrochemical Discharge Machining Process. *Arab J Sci Eng* 2021; 46: 2269–2281.

[13] QUTABA S, AZHARI A, ASMELASH M, et al. Development of Fiber Metal Laminate Composite with Different Glass Fiber GSM. Mater Today Proc. Epub ahead of print 2023.

[14] KULKARNI A, SHARAN R, LAL GK. An Experimental Study of Discharge Mechanism in Electrochemical Discharge Machining. I*nt J Mach Tools Manuf* 2002; 42: 1121–1127.

[15] KAMARAJ AB, JUI SK, CAI Z, et al. A Mathematical Model to Predict Overcut during Electrochemical Discharge Machining. *Int J Adv Manuf Technol* 2015; 81: 685–691.

[16] JAWALKAR CS. Investigation on Performance Enhancement of ECDM Process

while Machining Glass. *Indian Inst Technol Roorkee, India*

[17] JAWALKAR CS, SHARMA AK, KUMAR P. Experimental Investigations on Performance of ECDM using Design of Experiment Approach. i-manager's J Mech Eng 2011; 1: 24.

[18] SYED MH, QUTABA S, SYED L, et al. Greenly Prepared Antimicrobial Cotton Fabrics using Bioactive Agents from Cupressaceae Pods. *Surf Innov* 2022; 40: 1–13.

[19] BIN TARIQ SQ, SIDDIQUI Q, REHAN AM. Enhancement of Anti-Microbial Activity by Natural Finishes Prepared From Herbal Spices and Wastage Peel of Fruits Applied on Textile Substrate. *IOP Conf* Ser Mater Sci Eng 2018; 414: 012050.

[20] ANTIL P. Modelling and Multi-Objective Optimization during ECDM of Silicon Carbide Reinforced Epoxy Composites. *Silicon* 2020; 12: 275–288.

[21] N S, HIREMATH SS, J S. Prediction of Material Removal Rate using Regression Analysis and Artificial Neural Network of ECDM Process. *Int J Recent Adv Mech Eng* 2014; 3: 69–81.

[22] GANAPATHY S, BALASUBRAMANIAN P, VASANTH B, Et al. Comparative investigation of Artificial Neural Network (ANN) and Response Surface Methodology (RSM) expectation in EDM parameters. *Mater Today Proc* 2021; 46: 9592–9596.

[23] ABUZIED HH. Prediction of Electrochemical Machining Process Parameters using Artificial Neural Networks. 2012; 4: 125–132.

[24] SINGH T, KUMAR P, MISRA JP. Modelling of MRR during Wire-EDM of Ballistic Grade Alloy using Artificial Neural Network Technique. *J Phys Conf Ser*; 1240. Epub ahead of print 2019. DOI: 10.1088/1742-6596/1240/1/012114.

[25] ABRO ZA, HONG C, ZHANG Y, et al. Development of FBG Pressure Sensors using FDM Technique for Monitoring Sleeping Postures. *Sensors Actuators A Phys* 2021; 331: 112921.

[26] GUO S, ZHENG H, LIU X, et al. Comparison on Milling Force Model Prediction of New Cold Saw Blade Milling Cutter Based on Deep Neural Network and Regression Analysis. *Manuf Technol* 2021; 21: 456–463.

[27] ZHOU W, KANG M, GUO H. Development of a Surface Roughness Prediction Model for Slow Tool Servo Turning Machining. *Manuf Technol* 2022; 22: 111–122.

[28] WANG C, LI K, HU X, et al. Numerical Study on Laser Shock Peening of TC4 Titanium Alloy based on The Plate and Blade Model. *Opt Laser Technol* 2021; 142: 107163.

[29] SABAHI N, RAZFAR MR. Investigating The Effect of Mixed Alkaline Electrolyte (NaOH + KOH) on The Improvement Of Machining Efficiency In 2D Electrochemical Discharge Machining (ECDM). *Int J Adv Manuf Technol* 2018; 95: 643–657.

[30] KANTOR M, CHALUPA M, SOUČEK J, et al. Application of Genetic Algorithm Methods for Water Turbine Blade Shape Optimization. *Manuf Technol* 2020; 20: 453–458.

[31] KOLHEKAR KR, SUNDARAM M. A Study on the Effect of Electrolyte Concentration on Surface Integrity in Micro Electrochemical Discharge Machining. *Procedia CIRP* 2016; 45: 355–358.

[32] ZHANG W. Assembly Sequence Intelligent Planning Based on Improved Particle Swarm Optimization Algorithm. *Manuf Technol* 2023; 23: 557–563.

[33] JAHAN MP, RAHMAN M, WONG YS. A review on The Conventional and Micro-Electrodischarge Machining of Tungsten Carbide. *Int J Mach Tools Manuf* 2011; 51: 837–858.

[34] SAXENA KK, BELLOTTI M, VAN CAMP D, et al. Electrochemical Based Hybrid Machining. Elsevier Ltd. Epub ahead of print 2018.

[35] TARIQA SQBIN, SYEDA L, ZHAOLINGB LI. Evolution of Eco-Friendly Antimicrobial Finishes Extracted from Citrus Fruits Peel For textile Cotton Fabric with Furtherance Domestic Washing.

[36] ZHU Z, DHOKIA VG, NASSEHI A, et al. A Review of Hybrid Manufacturing Processes - State of The Art and Future Perspectives. *Int J Comput Integr Manuf* 2013; 26: 596–615.

[37] ZARE CHAVOSHI S. Analysis and Predictive Modeling of Performance Parameters in Electrochemical Drilling Process. *Int J Adv Manuf Technol* 2011; 53: 1081–1101.

[38] KUMAR KASDEKAR D, PARASHAR V, ARYA C. Artificial Neural Network Models for The Prediction of MRR in Electro-Chemical Machining. *Mater Today Proc* 2018; 5: 772–779.

[39] GUANG W, BARALDO M, FURLANUT M. Calculating Percentage Prediction Error: A User's Note. *Pharmacol Res* 1995; 32: 241–248.

[40] KIM S, KIM H. A New Metric of Absolute Percentage Error for Intermittent Demand Forecasts. *Int J Forecast* 2016; 32: 669–679.

[41] PHAM H. A New Criterion for Model Selection. *Mathematics* 2019; 7: 1–12.

[42] HAGAN MT, DEMUTH HB, BEALE M. Neural Network Design. PWS Publishing Co., 1997.

[43] QUTABA S, ASMELASH M, AZHARI A. Investigation on The Multiple Plies Structure of Aluminum-Lithium Alloy and Glass Fiber Composite with Respect To Deformation Failure. *Mater Res Express* 2023; 10: 016507.

[44] KONNO H, YAMAZAKI H. Mean-Absolute Deviation Portfolio Optimization Model and its Applications to Tokyo Stock Market. *Manage Sci* 1991; 37: 519–531.

[45] LI JG, YAO YX, GAO D, ET AL. Cutting Parameters Optimization by using Particle Swarm Optimization (PSO). In: *Applied Mechanics and Materials*. Trans Tech Publ, 2008, pp. 879–883.

[46] D'URSO G, RAVASIO C. Investigation on The Effects of Exchanged Power and Electrode Properties on Micro EDM Drilling of Stainless Steel. *Manuf Technol* 2019; 19: 337–344.

[47] GOUD M, SHARMA AK, JAWALKAR C. A Review on Material Removal Mechanism in Electrochemical Discharge Machining (ECDM) and Possibilities To Enhance The Material Removal Rate. *Precis Eng* 2016; 45: 1–17.

[48] NGUYEN KH, LEE PA, KIM BH. Experimental Investigation of ECDM for Fabricating Micro Structures Of Quartz. *Int J Precis Eng Manuf* 2015; 16: 5–12.